

Study of Nanoparticles at UTSA: One Year of Using the First JEM-ARM200F Installed in USA

Alvaro Mayoral^{†,†††}, Rodrigo Esparza[†], Francis Leonard Deepak^{†,††}, Gilberto Casillas[†], Sergio Mejía-Rosales^{††††}, Arturo Ponce[†] and Miguel José-Yacamán[†]

[†] Department of Physics and Astronomy, University of Texas at San Antonio

^{††} International Iberian Nanotechnology Laboratory, Avda Mestre Jose Veiga

^{†††} Laboratorio de Microscopías Avanzadas (LMA), Instituto de Nanociencia de Aragón (INA), Universidad de Zaragoza, c/Mariano Esquillor, Edificio I+D

^{††††} Center for Innovation and Research in Engineering and Technology, and CICEFIM-Facultad de Ciencias Físico-Matemáticas, Universidad Autónoma de Nuevo León

Contents

Study of Nanoparticles at UTSA: One Year of Using the First JEM-ARM200F Installed in USA	1
Exploring Biological Samples in 3D Beyond Classic Electron Tomography . . .	6
Application of Scanning Electron Microscope to Dislocation Imaging in Steel	11
Atmospheric Scanning Electron Microscopy (ASEM) Realizes Direct EM-OM Linkage in Solution: Aqueous Immuno-Cytochemistry	17
Information Derived from PGSE-NMR ~Ion Diffusion Behavior, Molecular Association, Molecular Weight/Composition Correlation of Synthetic Polymers~	23
Development of JEM-2800 High Throughput Electron Microscope.	31
Introduction of New Products	37

Cover micrograph

HAADF-STEM image of a gold decahedral particle oriented near a five-fold axis. Around the particle a cobalt oxide layer is growing. One of the (110) facets of the nanoparticles shows the 1 × 2 surface reconstruction corresponding to a missing atom row. Cobalt atoms occupy the empty gold atom positions. This is probably one of the best examples of epitaxial growth. (See page 5)

The first results from our group that have been obtained using the newly installed aberration-corrected STEM microscope (JEOL JEM-ARM200F) are reported. Studies were carried out on noble metal nanoparticles and their corresponding alloys and/or core-shell structures. In this paper we focus on some of the exciting areas of research that have been under investigation in our group. These include studies on Au nanoparticles, bimetallic Au-Co nanoparticles and core-shell Au-Pd nanoparticles. In addition, studies that were carried out on very small clusters namely Pd-Ir and other similar systems have also been highlighted in this report.

Introduction

The University of Texas at San Antonio organized recently an Electron Microscopy core facility named the "Kleberg Advanced Microscopy Facility". The most relevant instrument is a JEOL JEM-ARM200F (with FEG) with probe aberration correction; this instrument was the first one installed outside Japan and is operational since February 2010. In this paper we report some of the results after one year of its operation.

Experimental

For the electron microscopy analysis, the nanoparticles samples were dispersed in ethanol and a drop of this suspension was deposited onto a holey carbon grid. The samples were characterized using the aberration (C_s) corrected JEOL JEM-ARM200F (ARM) 200 kV FEG-STEM/TEM, equipped with a CEOS C_s corrector on the illumination system. The probe correction was performed through a dodecapole corrector (CEOS GmbH) aligned through the

CESCOR software, to finally obtain a twelve-fold Ronchigram with a flat area of 50 mrad. The pixel spacing was calibrated using Si [110] lattice images in the HAADF mode, and confirmed by using gold standard particles. Images were commonly recorded for 10 to 16 s. The probe current used for acquiring the HAADF as well as the BF-STEM images was 9C (23.2 pA) and the CL aperture size was 40 μ m. High angle annular dark-field (HAADF) STEM images were acquired with a camera length of 8 cm/6 cm and the collection angle of 50-180 mrad/67-250 mrad was used. The BF-STEM images were obtained using a 3 mm/1 mm aperture and a collection angle of 11 mrad/3.8 mrad was used (camera length in this case was 8 cm). The HAADF as well as the BF images were acquired using a digiscan camera. In order to reduce the noise of the images and to obtain clearer images the raw data was filtered using the 2D Wiener filter and the Richardson-Lucy/Maximum Entropy algorithm implemented by Ishizuka. The EDS analysis was performed using EDAX instrumentation attached to the JEOL-ARM microscope. Spectra, line scans as well as chemical maps for the various elements were obtained using the EDAX Genesis software. For the EDS analysis the probe size used was 6C (145 pA) and the CL aperture size was 40 μ m. One- and two-dimensional elec-

One UTSA Circle, San Antonio, Texas 78249, USA

miguel.yacaman@utsa.edu



tron energy loss spectroscopy (EELS) analysis was performed with a GIF-Tridiem spectrometer. The probe size used was 6C (145 pA) and the CL aperture size was 40 μm (camera length – 6 cm).

Results and Discussion

Monometallic nanoparticles

Nanoparticles are a fundamental part of nanotechnology. In fact, metal nanoparticles were used since the 1940's to improve the quality of gasoline. The surprisingly high catalytic activity of particles in the nano size range was recognized early and hence it was used extensively [1]. However, for many years it was assumed that the only role of the particles was to provide a higher surface area. The recent explosion of interest in nanotechnology has made clear the fundamental physical principles behind the particle behavior. The nanoparticles are intermediate between clusters (a few atoms) and bulk systems. In fact clusters are different from nanoparticles in the fact that most of the atoms are on the surface. In a particle although an important fraction of the atoms are on the surface there is still a core of non-surface atoms.

The use of HAADF-STEM has opened up new and exciting possibilities to understand nanoparticles. The atomically resolved images in combination with EDS and EELS data provide a very powerful set of tools capable of understanding the atomic behavior.

One of the most common findings in nanoparticles is that the crystal structure is different from that of the bulk. The most commonly observed case is the formation of the five fold symmetry structures such as the icosahedron and decahedron [2-4]. A very fundamental problem is to understand how these structures become stable. **Fig. 1** shows

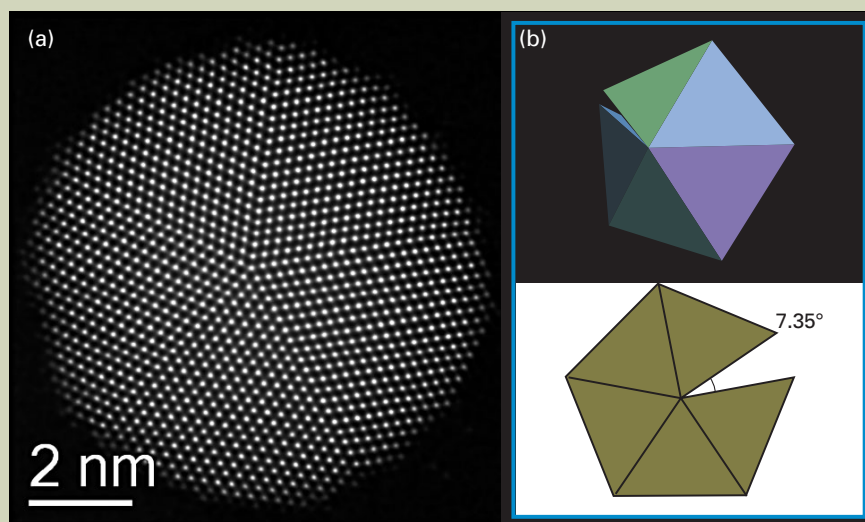


Fig. 1 (a) Au decahedra oriented along the 5-fold axis of the particle, (b) geometry angular deficiency in the decahedra. For a decahedron, the angle between adjacent (111) plane is 7.35° on projection of (110) orientation.

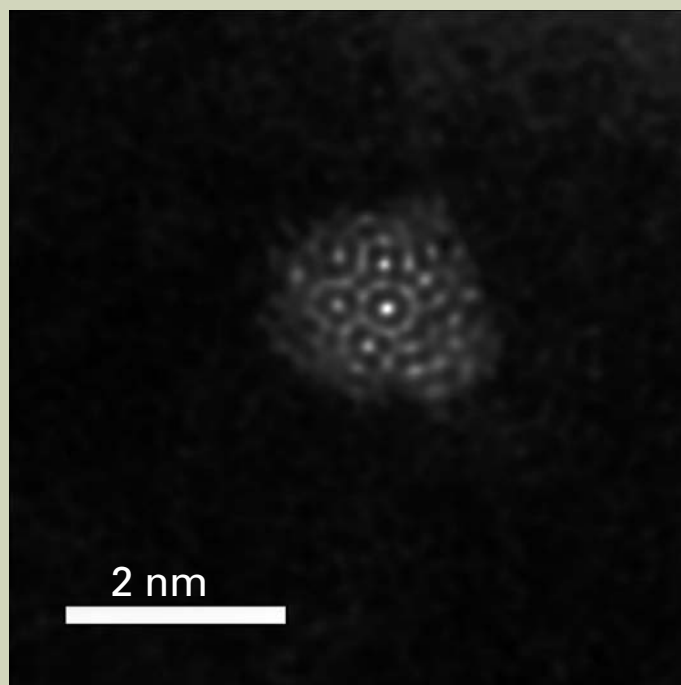


Fig. 2 The smallest icosahedra observed so far in which the five-fold symmetry is apparent.

an example of a gold decahedral particle in which the atomic columns are revealed by the HAADF-STEM image. A periodic strain can be observed along the one of the twin boundaries and this is related to the fact that if we pack five fcc regular tetrahedra in a cyclic twinning (see Fig. 1b) a gap of $7^\circ 35'$ will be produced. The strain on the particle will be necessary to accommodate the gap. It is possible from images of this kind, to measure the strain more accurately. In **Fig. 2**, we show one of the smallest icosahedra so far observed in which the fivefold symmetry is apparent.

Bimetallic nanoparticles

The properties of metallic nanoparticles can be improved by adding a second metal [5].

Indeed many of the most useful nanoparticles are bimetallic, one important problem is to determine its detailed structure and chemical composition. In our group since the last few years we have been carrying out a very extensive research program on bimetallic nanoparticles. We have studied a number of systems including Au/Pd, Au/Co, Au/Pt, Pd/Pt and Au/Ag among many others. Normally it is assumed [2] that nanoparticles with two metals will show a structure which is either core-shell or an alloy. In the first case, one metal will be the core and the second metal will be the shell surrounding the core. However experimental results from our group clearly indicate [6, 7] that the structure is much more complex, than a simple alloy or core shell structure. We will describe these details in the following sections.

Z contrast

When studying nanomaterials with two different elements, the most interesting case being those of transition and noble metals, the TEM techniques are somewhat limited since the contrast is more related to coherent scattering. Thus one of the major limitations is the diffraction contrast which will be easily observed (if present). Bright field images might give some information if there is strain or change of orientation between the core and shell structure. However, STEM-HAADF is the most important technique in the study of bimetallic nanoparticles. The intensity of the signal which is generated

will be proportional to the atomic number and the contrast due to the atomic composition will be clearly observed. In order to illustrate this effect we have made calculation of the intensity of columns of atoms of different elements with the same number of atoms. We have carried out multislice calculations using the software developed by HREM Inc.[8] The results are shown in **Figs. 3(a)** and (b). We have plotted a relative contrast of a number of elements where the Z contrast is apparent. On the other hand the intensity goes as $I \sim Z^{1.45}$. With the probe corrected aberration a resolution of 0.8 Å can be achieved therefore variations of the composition at atomic scale can be observed.

Experimental examples of bimetallic particles

When applied to real nanoparticles that have been obtained in our laboratory, the atomic contrast is clearly observed. **Fig. 4** (a) and (b) shows an Au/Pd nanoparticle grown by chemical synthesis (6). The variation in the composition is clearly observed (Fig.4(b)), the central core is an alloy rich in Pd, then a second layer of alloy rich in gold and finally a exterior shell which is an alloy rich on Pd. It is possible to plot the chemical composition along the particle using EDS and EELS, the result of which is shown in **Fig. 5** and **Fig.6**. EDS line scan in the case of the three-layer Pd-Au-Pd nanoparticles

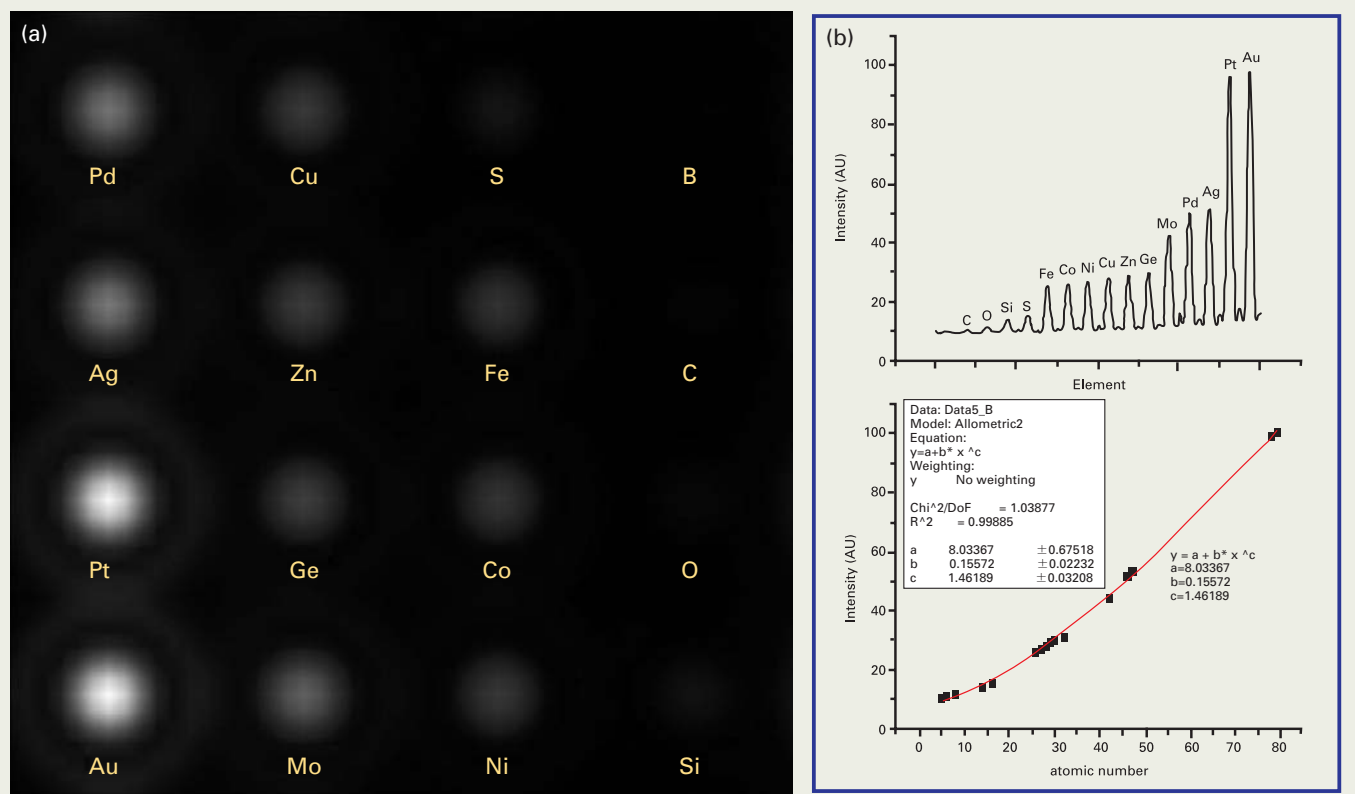


Fig. 3 (a) Calculations of the relative HAADF-STEM contrast of different elements (columns with the same number of atoms). The atomic number contrast is very clear, (b) Variation of the intensity of the contrast with the atomic number.

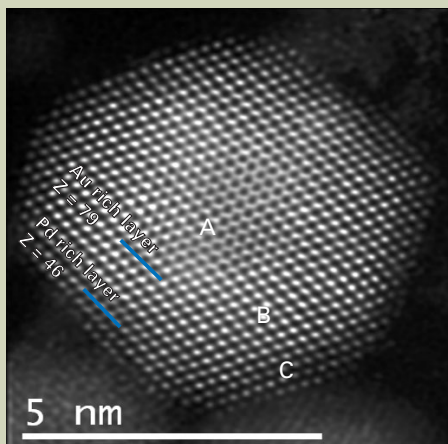


Fig. 4 A truncated cuboctahedra three-layered (Pd-Au-Pd) nanoparticle.

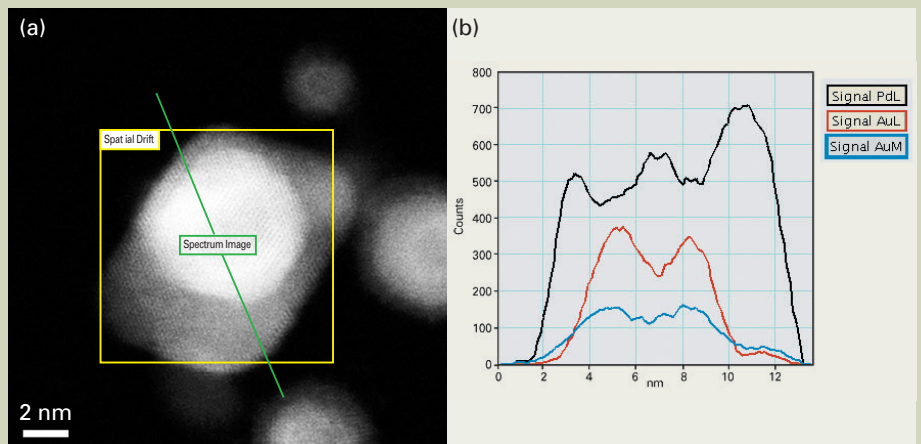


Fig. 5 (a) and (b) Characterization of the Au and Pd elemental distribution across the nanoparticle by STEM-EDS line-scanning technique across the individual three-layer nanoparticle. The Pd-L and the Au-L,M line scan signals can be clearly seen varying in intensity along the different regions of the nanoparticles. (a) Shows the analyzed area and the direction of analysis.

reveal the following interesting features as can be seen in Fig. 5. The Pd-L and the Au-L,M signals can be clearly traced across the region of the individual Pd and Au layers with the maximum intensity of the signals varying between the respective layers (Fig. 5(b)). The corresponding EELS map of Pd reveals clearly the presence of Pd in the core and in the outermost shell of the tri-layered nanoparticles as is shown in Fig. 6. These results clearly confirm the complex chemical nature of the bimetallic particles. In addition it is possible even to distinguish layer by layer, when it is Pd rich or Au rich as shown in Fig. 7. Thus it is worthy to mention that in case of these nanoparticles occasionally four-layered structure are seen.

Shown in Fig. 7, is the case of the four layered nanoparticles wherein it can be seen that near the surface there is an extra layer of atoms of gold and this suggests a four layered structure. This is a different case from the previously mentioned three-layered nanoparticles and has not been reported till date.

A very interesting result is shown in Fig. 8, wherein two Au/Pd particles that have coalesced are forming an elongated structure. Most remarkably the 3 layer structure is preserved by the coalescence. This means that during the initial coalescence process the Pd atoms diffuse along the boundary. However many bright spots, corresponding to gold atoms can be observed on the region common

to the two particles.

Surface reconstruction in nanoparticles

One of the most interesting discoveries of the surface science research back in the seventies was that, the surfaces of crystals can have a different atomic arrangement than those of the bulk [9]. This phenomenon is known as surface reconstruction and in the mid 80's Marks *et al.* [10] showed that indeed surface reconstruction is also observed in gold nanoparticles. In our group we have been investigating the conditions in which surface reconstruction appears. We have observed inter-

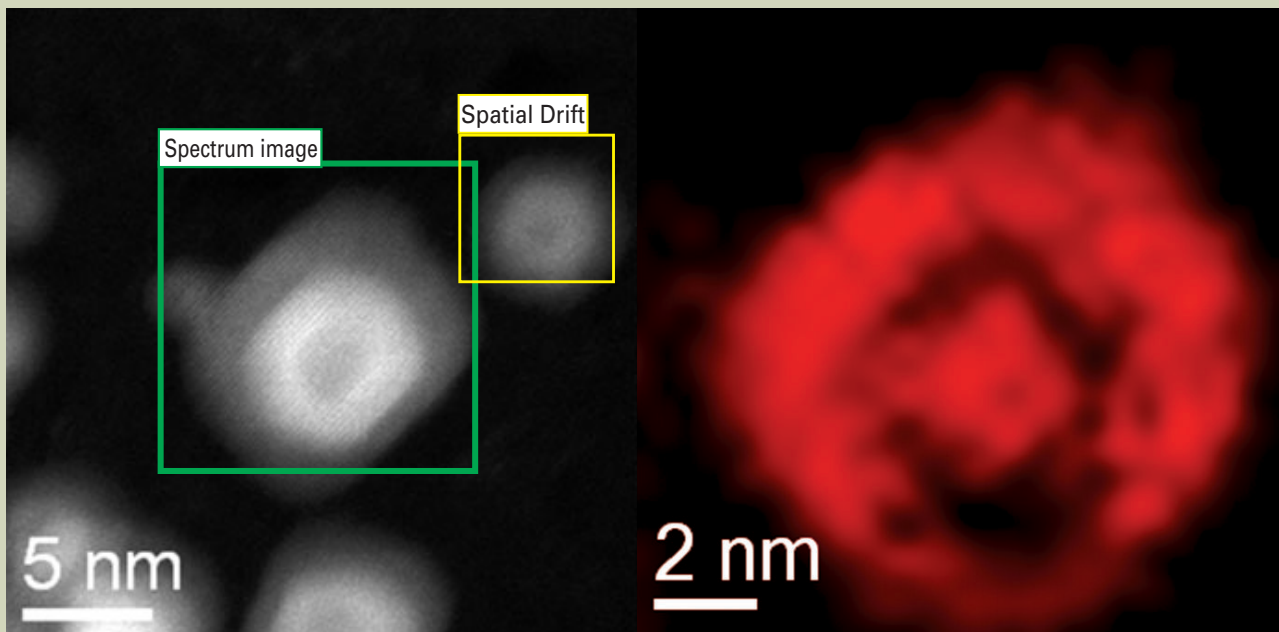


Fig. 6 EELS map of Pd reveals clearly the presence of Pd in the core and in the outermost shell of the tri-layered nanoparticles.

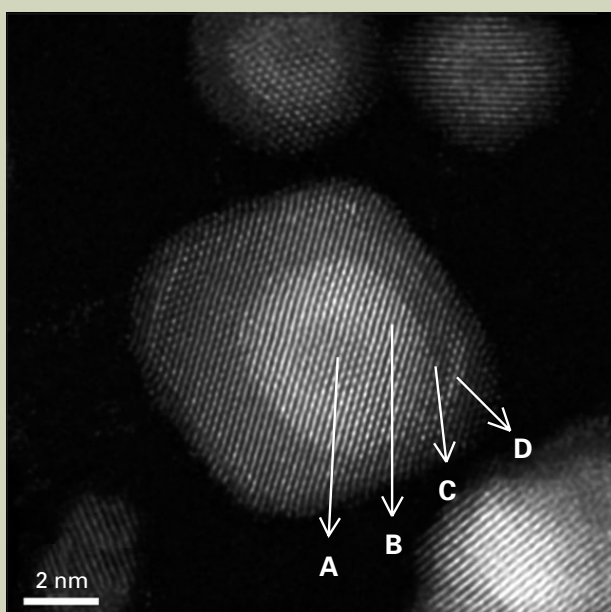


Fig. 7 Aberration-corrected STEM images of the four layered Au/Pd nanoparticles. The contrast of the four distinct regions (marked A, B, C and D) can be clearly seen.

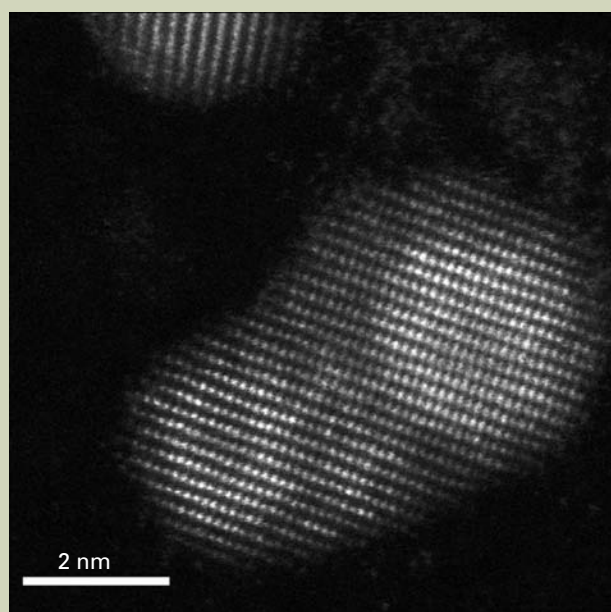


Fig. 8 Coalescence of two/three-layered Pd-Au-Pd nanoparticles. Notice also the Au intercalation into the Pd layer.

faces of Au with Co. Shown in **Fig. 9** (a) is the $\langle 110 \rangle$ surface of a Au/Co nanoparticle. The bright atoms correspond to gold and the light atoms correspond to Co. It can be observed that gold shows a (1×2) reconstruction. A model of the reconstructed surface in the missing row is shown in Fig. 9(b) (compare the image Fig. 9a and the model Fig. 9b). The interesting result is that 10 atoms accommodate on the places of the missing gold atoms. This kind of analysis suggests ways in which surfaces can be tailored for improved catalytic activity.

Observation of individual atoms/clusters

It is indeed interesting to note that the ultimate resolution of observing individual atoms/small clusters have been achieved using the ARM. Shown in **Fig. 10**, are the very small clusters of Pd-Ir (inside the circle). The size of the cluster is just about ~ 2 nm. It is interesting to note that based on the Z contrast, the two different atoms can be distinguished very clearly (Pd, $Z = 46$, Ir = 77). In addition in the vicinity of these small clusters it is also possible to locate individual atoms of Ir/Pd (outside the circle).

Conclusions

This paper summarizes the most important results on noble metal nanoparticles obtained

from our group over the last year with the new ARM microscope. It is clear from the discussion provided, on the results that have been obtained concerning metal nanoparticles/bimetallic and core-shell nanoparticles and other related systems, that it has indeed been an exciting one year. With unprecedented advantages in terms of resolution and using the HAADF-STEM imaging in combination with additional spectroscopic tools associated with it, namely EDS and EELS it has been possible to unravel some of the fundamental questions in the case of nanoparticles. Indeed with all these new developments, we can look forward to many such more exciting areas of research in the coming years.

Acknowledgements

The authors would like to acknowledge THE WELCH FOUNDATION AGENCY PROJECT # AX-1615. "Controlling the Shape and Particles Using Wet Chemistry Methods and Its Application to Synthesis of Hollow Bimetallic Nanostructures". The authors would also like to acknowledge the NSF PREM Grant # DMR 0934218, Title: Oxide and Metal Nanoparticles - The Interface between life sciences and physical sciences. The authors would also like to acknowledge RCM Center for Interdisciplinary Health Research CIHR. The project described was supported by Award Number

2G12RR013646-11 from the National Center for Research Resources. The content is solely the responsibility of the authors and does not necessarily represent the official views of the National Center for Research Resources of the National Institutes of Health. Finally, the authors would like to thank Dr. Eduardo Pérez-Tijerina from UANL for providing of some of the samples included in this paper.

References

- [1] G. Somorjai, *Chem. Rev.*, **96**, 1223 (1996).
- [2] A. L. Mackay, *Acta Crystallogr.*, **15**, 916 (1962).
- [3] J. L. Rodriguez-Lopez, J. M. Montejano-Carrizales, M. Jose-Yacaman, *Modern Physics Letters*, **20**, 725 (2006).
- [4] L. D. Marks, *Reports on Progress in Physics*, **57**, 603 (1994).
- [5] R. Ferrando, J. Jellinek, R. L. Johnston, *Chem. Rev.*, **108**, 845 (2008).
- [6] D. Ferrer, D. A. Blom, L. F. Allard, *J. Mat. Chem.*, **18**, 2442 (2008).
- [7] D. Ferrer, A. Torres-Castro, X. Gao et al. *Nano Lett.*, **7**, 1701, 2007.
- [8] K. Ishizuka, N. Uyeda, *Acta Cryst. A*, **33**, 740 (1977).
- [9] H. Wagner. *Springer Tracts in Modern Physics (Springer, Berlin)*, **85**, (1979).
- [10] L. D. Marks, *Phys. Rev. Lett.*, **51**, 1000 (1983).

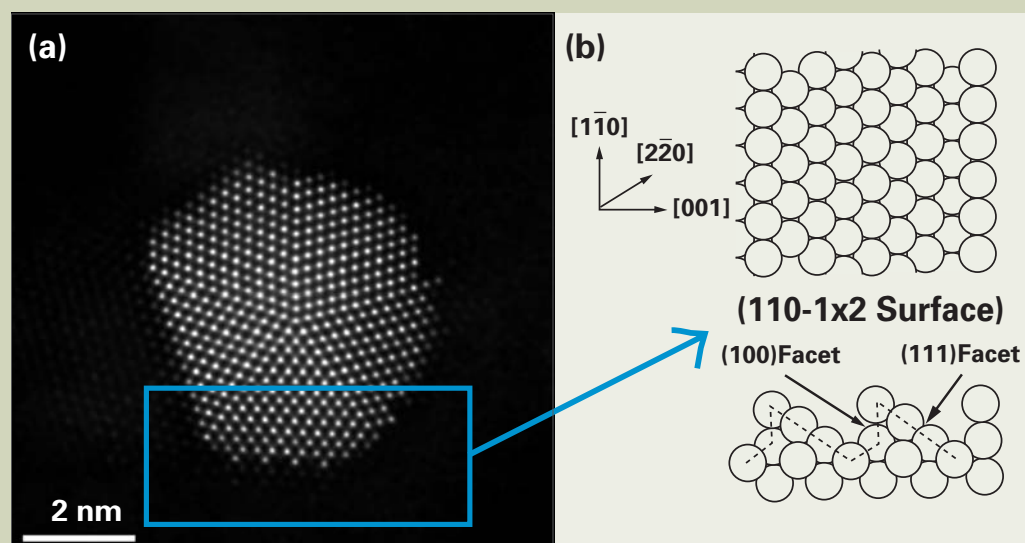


Fig. 9 (a) Image of surface reconstruction observed in Au-Co nanoparticles and (b) the corresponding model showing the 1×2 reconstruction.

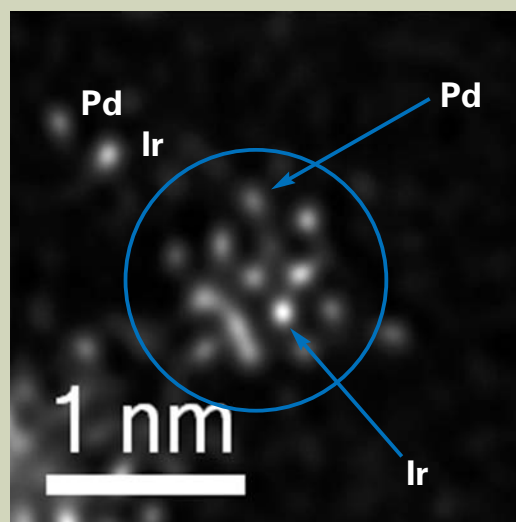


Fig. 10 Clusters of Pd-Ir are shown (inside the circle). It is possible to distinguish each element based on the Z contrast (Pd = 46, Ir = 77). Notice also the presence of individual atoms (outside and close to the circle).